The Cdi/TESK1 kinase is required for Sevenless signaling and epithelial organization in the *Drosophila* eye

Marta Sesé[1], Montserrat Corominas[1], Hugo Stocker[2], Tapio I. Heino[3], Ernst Hafen[2] and Florenci Serras[1,*]

[1]Departament de Genètica, Facultat de Biologia, Universitat de Barcelona, Diagonal 645, 08028 Barcelona, Spain
[2]Institute for Molecular Systems Biology, ETH Zürich, c/o Zoologisches Institut, Universität Zürich, Winterthurerstr. 190, 8057 Zürich, Switzerland
[3]Institute of Biotechnology and Department of Biological and Environmental Sciences, University of Helsinki, FIN-00014 Helsinki, Finland
*Author for correspondence (e-mail: fserras@ub.edu)

Accepted 10 October 2006
Journal of Cell Science 119, 5047-5056 Published by The Company of Biologists 2006
doi:10.1242/jcs.03294

Summary

How cellular behaviors such as cell-to-cell communication, epithelial organization and cell shape reorganization are coordinated during development is poorly understood. The developing *Drosophila* eye offers an ideal model system to study these processes. Localized actin polymerization is required to constrict the apical surface of epithelial cells of the eye imaginal disc to maintain the refined arrangement of the developing ommatidia. The identity of each photoreceptor cell within the epithelium is determined by cell-to-cell contacts involving signal transduction events. The R7 photoreceptor cell requires the activity of the Sevenless RTK to adopt a proper cell fate. We performed an EP screen for negative regulators of this inductive process, and we identified the serine/threonine kinase Center divider (*cdi*) as a suppressor of the phenotype caused by an activated Sevenless receptor. Cdi is homologous to the human testis-specific kinase 1 (TESK1), a member of the LIM kinases involved in cytoskeleton control through ADF/cofilin phosphorylation. We have analyzed the effects of gain- and loss-of-function of *cdi* and found alterations in actin organization and in the adherens junctions proteins DE-cadherin and β-catenin, as well as in Sevenless apical localization. Interference with the function of the ADF/cofilin phosphatase Slingshot (*ssh*), which antagonizes Cdi, also results in a suppression of signaling triggered by the Sevenless RTK. Our results reveal a critical interplay between the localization of molecules involved in epithelial organization and signal transduction.

Key words: cdi, Sevenless, Photoreceptor, Eye, Actin

Introduction

During development, epithelial tissues provide the structural framework where many morphogenetic events operate. Signaling pathways, cytoskeleton organization and cell polarity are known to be crucial for epithelial organization and cell shape in development. However, little is known about how these cellular activities are integrated to coordinate development. *Drosophila* eye development offers the possibility to study the link between signaling and cellular architecture, since cell differentiation requires cell-to-cell interactions in a tightly organized epithelium.

The organization of the *Drosophila* compound eye is initiated when a groove, called the morphogenetic furrow, sweeps the columnar epithelium of the imaginal disc from posterior to anterior (Ready et al., 1976; Wolff and Ready, 1991) and leaves the determined R8 photoreceptor founder cell behind it. The R8 photoreceptor precursor progressively recruits the other precursors of photoreceptor cells in an inductive event essentially triggered by the activation of the Ras/MAPK pathway mediated by the induction of the epidermal growth factor receptor (DER). The activation of the DER is sufficient to recruit R1 to R6 photoreceptors (Freeman, 1996) but the R7 photoreceptor cell requires the additional activation of a second receptor tyrosine kinase (RTK), the Sevenless (Sev) receptor (Tomlinson and Ready, 1986; Hafen et al., 1987; Basler and Hafen, 1988). In *sev* mutants, each R7 precursor cell fails to adopt a neuronal cell fate and assumes the cone cell fate instead (Tomlinson and Ready, 1986). *sev* is transiently expressed in a subpopulation of ommatidial precursor cells, the *sevenless* equivalence group (the precursors of R3, R4, R7, R1, R6 and cone cells), but is exclusively required in R7 (Tomlinson et al., 1987; Banerjee et al., 1987). The Sev RTK protein is mostly localized in the apical region of these cells where cell-to-cell contacts with the R8 founder cell occur (Banerjee et al., 1987; Tomlinson et al., 1987). The ligand of Sev RTK is the seven-pass transmembrane protein Bride of sevenless (Boss), which is localized in the apices of the R8 cell (Reinke and Zipursky, 1988; Hart et al., 1990). The precise spatio-temporal expression and localization of Boss is a prerequisite for the R7-precursor to activate the Sev RTK and assume the R7 fate (Van Vactor et al., 1991).

Photoreceptor cells are specified in an epithelium where the apical surfaces are tightly packed and constricted, probably to concentrate the receptors for signaling events (Tomlinson and Ready, 1987; Wolff and Ready, 1991). The intercellular junctional complex of the arthropods includes adherens junctions located at the most apical position on the lateral cell membrane (Woods et al., 1997). Adherens junctions hold epithelial cells together and provide strong mechanical attachments between adjacent cells. They are built of

cadherins, which are transmembrane proteins whose intracellular segments bind to catenins connected to actin filaments (reviewed by Tepass et al., 2001). Regulators of the apical-basal polarity and the integrity of the adherens junctions, have a distinct role in photoreceptor morphogenesis (Izaddoost et al., 2002; Pellikka et al., 2002). Moreover, some elements associated with structural components of the cell appear to be required for R7 fate. For example, the membrane skeleton protein βH-spectrin, which in its tetrameric form crosslinks actin, is essential for the correct development of R7, as mutants for βH-spectrin result in missing R7 (Thomas et al., 1998).

The epithelial organization requirement for photoreceptor specification can be bypassed by the constitutive activation of signal transduction pathways. A gain of Sev function (sev^{S11}) was achieved by overexpressing an N-terminally truncated Sev protein under the control of the duplicated *sev* enhancer fragment. This construct lacks most of the extracellular domain and ensures the temporal and spatial expression pattern of *sev* (Basler et al., 1991). This constitutive activation of Sev is sufficient to specify R7 cell fate not only in the R7 precursor but also in other cells of the equivalence group, resulting in rough eye phenotype (Basler et al., 1991).

In a sensitized misexpression screen for EP lines modifying the rough eye phenotype of sev^{S11}, we found *center divider* (*cdi*) as a suppressor. *cdi* encodes a serine/threonine kinase orthologous to mammalian testis-specific kinase 1 (TESK1) (Matthews and Crews, 1999). The protein kinase domain of TESK1 is structurally similar to domains of LIMK1 (Toshima et al., 1995) and stimulates the formation of actin stress fibers and focal adhesions through phosphorylation of F-actin depolymerizing factor ADF/cofilin (Toshima et al., 2001a). ADF/cofilin is reversibly activated by phosphatases and inhibited by kinases (Niwa et al., 2002; Ghosh et al., 2004; DesMarais et al., 2005; Gohla et al., 2005). We show that Cdi is required for the correct signaling activity of the Sev pathway as well as for the cellular organization of the developing eye. This work provides evidence for a link between signaling and cytoskeletal organization and polarity of the epithelium, which act in conjunction to fine tune the signal transduction events that lead to the specification of photoreceptor cells.

Results

cdi as a suppressor of the activated Sevenless pathway

To identify negative regulators of the Sev RTK-activated signaling pathway, we carried out a misexpression screen for genes that suppress a rough eye phenotype caused by the constitutively activated form of the Sev receptor, sev^{S11}. This activated form, which is expressed in *sevenless* equivalence group cells, resulted in a characteristic rough eye of irregular ommatidia due to extra R7 photoreceptors per ommatidium (Basler et al., 1991). We tested 5000 fly lines containing random insertions of a double-headed enhancer-promoter (EP) element carrying 3′UAS and 5′UAS sites that permit the transcription of genes flanking the insertion in response to Gal4 (Fig. 1C). Flies carrying both the sev^{S11} construct and the *sev-Gal4* driver were crossed to those EP lines. Several independent lines were identified as suppressors of the activated Sev pathway, among them *EP(33-077)*, *EP(44-004)* and *EP(34-165)* that clustered in the 91F region of the third chromosome very close to each other (Fig. 1A-B). To determine whether the suppression was due to the EP insertion site, each EP line was crossed to sev^{S11} flies in the absence of *sev-Gal4*, and no suppression could be observed (Fig. 1D). Then, for each EP line, the 5′ UAS site was excised by Cre-loxP-mediated recombination to yield a single-headed $EP(y^{-})$ element (Fig. 1C). The resulting $EP(44\text{-}004y^{-})$ and $EP(34\text{-}165y^{-})$ lines were still strongly suppressing the sev^{S11} rough eye phenotype (Fig. 1D). Three genes are located in the vicinity of the EP insertion sites: *ATP synthase*, *subunit d* (*ATPsyn-d*), *mitochondrial ribosomal protein L55* (*mRpL55*) and *center divider* (*cdi*) (Fig. 1E). However, all three EP lines were oriented with the 3′ UAS site driving the expression of both *mRpL55*, which has been described as a ribosomal protein implicated in cell cycle progression (Dimova et al., 2003), and *cdi*, which is expressed in the embryonic midline of the *Drosophila* central nervous system (Muralidhar et al., 1993; Matthews and Crews, 1999). To corroborate transcriptional induction of both genes through the EPs, we tested the EP lines by RT-PCR after activation of a heat shock driven Gal4, and found an increase of the transcription of both *cdi* and *mRpL55* genes in double and single-headed EP lines (Fig. 1F), whereas *ATPsyn-d*, which is in opposite orientation, did not show any change of expression (not shown).

Since those two genes in tandem were activated by the EPs, we used *UAS-cdi* and *UAS-mRpL55* transgenes to find out which of them is responsible for the suppression or whether they both contribute to it. We found that *UAS-cdi* recapitulated the suppression of sev^{S11} phenotype, whereas *UAS-mRpL55* did not. In the absence of *UAS-cdi* activation, the average of the number of R7 cells per ommatidium was 4.3, and this number dropped to 3.3 in the presence of the *sev-Gal4* driver (Fig. 2A).

To exclude some contribution of *mRpL55*, *UAS-mRpL55* construct was activated together with *UAS-cdi* and no enhancement of the sev^{S11} suppression was observed (data not shown). To determine whether both the EP lines and the *UAS-cdi* are capable of driving expression of the Cdi protein, we activated them with an *en-Gal4* line in the wing disc and found strong Cdi localization in the posterior compartment after staining with anti-Cdi (Fig. 1G,H).

To examine the specificity of *cdi* as a suppressor of the *sevenless* pathway, we used *UAS-boss* as an independent construct to activate the signaling pathway. Overexpression of the ligand Boss in the *sevenless* equivalence group cells results in an expanded ligand-receptor interaction and therefore more R7 cells in 80% of the ommatidia (Fig. 2B) with an average of 2.7 R7 cells per ommatidium. When we overexpressed *cdi* in this context, even with only one copy of the *UAS-cdi* transgene, we observed that the average number of R7 per ommatidium dropped to 1.9 (Fig. 2B). In some of these ommatidia no R7 was detected (<5% in Fig. 2B), which suggests that overexpression of *cdi* can interfere with R7 formation. To test this, we analyzed flies carrying *sev-Gal4 UAS-cdi* constructs in a wild-type background and found that in 3% of the ommatidia the R7 cell was absent (inset in Fig. 2B).

To analyze *cdi* expression in the wild-type eye disc we used an antibody against the Cdi protein. At the third instar we found extensive localization throughout the eye-antenna disc. The localization of Cdi was cytoplasmic and more prominent in the apical domains of the eye disc epithelium, as seen in transverse sections of both photoreceptor precursors and surrounding cells (Fig. 3A-D). To analyze whether the

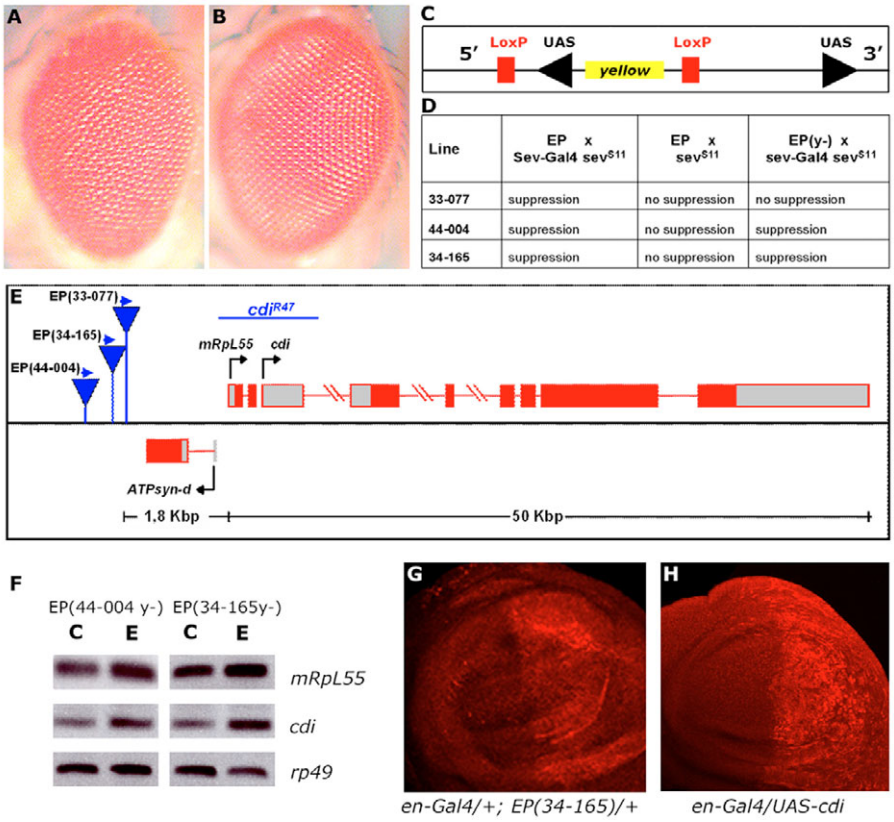

Fig. 1. The *EP(33-077)*, *EP(44-004)* and *EP(34-165)* suppression of the rough eye phenotype when Sev RTK signaling is activated. (A) Rough eye phenotype caused by the constitutively activated Sev receptor (sev^{S11}/+). (B) Suppression of the rough eye phenotype due to the overexpression of a double-headed EP line identified in the screen (*sev-Gal4* sev^{S11}*/EP*). Note that the regular pattern of ommatidia is rescued. (C) The double-headed EP transposable element, showing the 5′ and 3′ UAS sites (black arrowheads). Activation of the Gal4 drives expression of the genes adjacent to 5′ and 3′ UAS sites. The loxP sites flanking the 5′ UAS (red boxes), will remove the 5′ UAS site when in the presence of the recombinase *cre*. Note that flies lacking the 5′ UAS site will be distinguished by the lack of the $yellow^{+}$ marker and named $EP(y^{-})$. (D) Summary of the suppression of the Sev^{S11} construct by the three EP lines. (E) Genomic region and insertion of *EP(33-077), EP(44-004)* and *EP(34-165)*. There are three genes in this region: *ATPsyn-d*, *mRpL55* and *cdi.* Black arrows indicate the transcription starts and orientation of the three genes. The *EP(33-077)* is 1.800 bp upstream from 5′ UTR of *mRpL55*. They are orientated with the 3′ UAS site (small blue arrows) towards the 5′ end of *cdi* and *mRpL55*. The blue bar represents the 2.077 bp deletion of the cdi^{R47} allele. (F) Molecular characterization of the gene expression induced by the EP lines. RT-PCR from *hs-Gal4 EP* larvae after heat shock induction indicates that both *cdi* and *mRpL55* transcripts are overexpressed. $EP(34\text{-}165y^{-})$ and $EP(44\text{-}004y^{-})$ are shown as examples, and *rp49* expression as a control. C lanes show expression without heat shock. E lanes show expression after heat shock. (G) Wing disc from *en-Gal4/+; EP 34-165/+* larvae stained with an antibody against Cdi. Cdi protein is strongly expressed in the posterior compartment due to EP activation. (H) *en-Gal4/UAS-cdi* wing discs stained with anti-Cdi show abundant localization of Cdi in the posterior compartment.

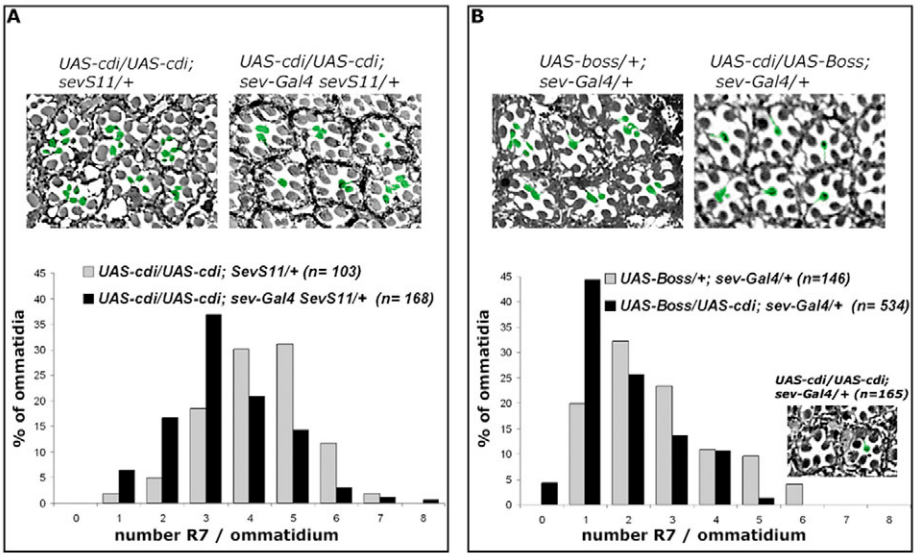

Fig. 2. *cdi* as a suppressor of the activated Sev pathway. (A) Semi-thin section from a control eye (left) where *UAS-cdi* is not overexpressed (*UAS-cdi/UAS-cdi;* sev^{S11}/+) and an experimental eye (right) where the *UAS-cdi* is overexpressed by *sev-Gal4* (*UAS-cdi/UAS-cdi; sev-Gal4* sev^{S11}/+). The histogram shows distribution profiles of the number of R7 photoreceptors per ommatidium for each genotype represented. The statistical analysis reveals significant differences between the genotypes (P<0.001). (B) Semi-thin section of control eye (left), where *UAS-Boss* is expressed under *sev-Gal4* (*UAS-Boss/+; sev-Gal4/+*) and experimental eyes (*UAS-cdi/UAS-Boss; sev-Gal4/+*) are shown. The histogram quantifies the number of R7 per ommatidium with and without *cdi* overexpression (P<0.001). The inset below shows two ommatidia from a *UAS-cdi/UAS-cdi; sev-Gal4* fly, one with R7 (right) and one without (left). R7 rhabdomeres are colored green.

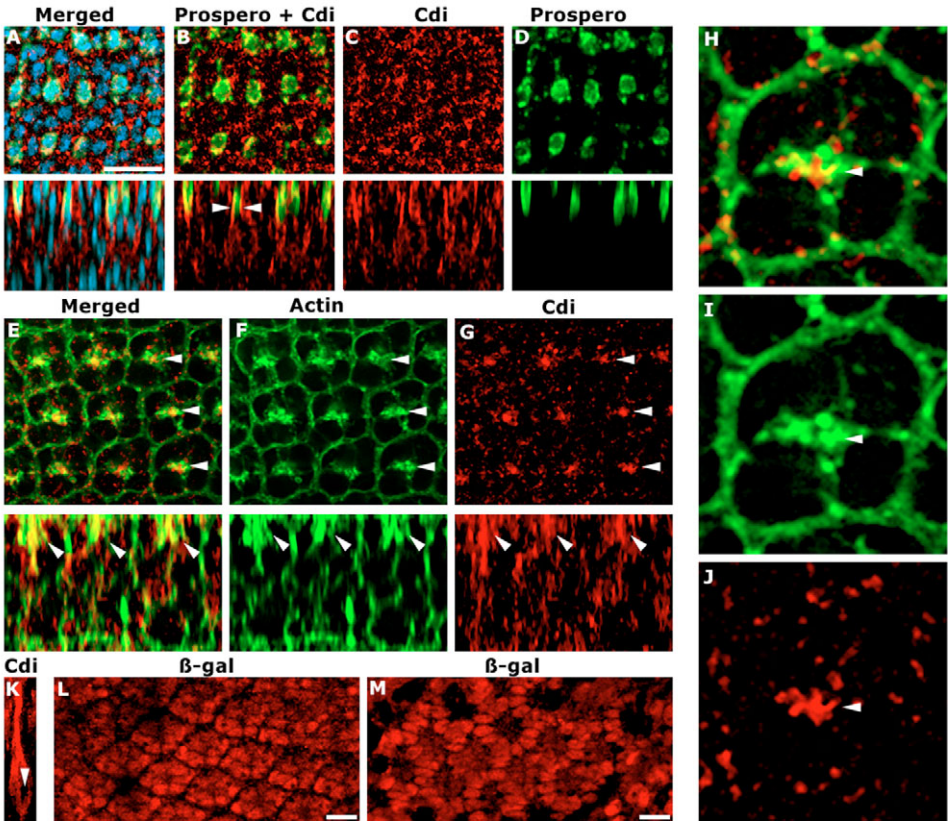

Fig. 3. *cdi* expression pattern in the eye imaginal disc. (A-D) Cdi pattern (red) of a disc co-stained with prospero (green). The confocal image was captured at the level of the R7 cells to discriminate from the prospero-stained cone cells. Upper panels: cross-section. Lower panels: transverse section. Arrowheads point to the localization of R7 cells. The merged figure in A also shows nuclear staining with Sytox-green (blue) to show distribution of nuclei. Note that in the transverse XZ sections (lower panels) the localization of Cdi is more abundant in the apical region of the epithelium (top). (E-G) Co-localization of F-actin (green) and Cdi (red) in the apical constrictions. Arrowheads point to apical constrictions. Upper panels: optical section taken through the most apical domain of the eye disc. Lower panels: transverse sections. (H-J) High magnification of an ommatidium of the previous image, showing Cdi (red) in the F-actin enriched apical constriction (green). (K) High magnification of a transverse section of a pupal photoreceptor to show cytoplasmic localization of Cdi. Apical: top. Arrowhead points to the nucleus. (L-M) Two confocal planes of developing ommatidia of a cdi^{BA01} early pupal disc stained with anti β-galactosidase. Labeling is extensive throughout the ommatidial cells. Bars, 10 μm.

precursor of the R7 photoreceptor also expressed Cdi, we co-stained these discs with an antibody to the nuclear protein Prospero and detected Cdi in the cytoplasm of the R7 cells (Fig. 3A-D). The apical surfaces of the ommatidial cluster cells remain constricted and they are enriched with F-actin (Tomlinson et al., 1987). To examine whether these apical constrictions also contain Cdi, we co-stained eye discs with phalloidin and anti-Cdi. In addition to the cytoplasmic localization, an accumulation of Cdi was found in the apical tips of the clusters at late third instar and early pupal stages and this accumulation overlapped with the F-actin-rich apical constrictions (Fig. 3E-J). A transient accumulation of Cdi in the R8 precursor was also found in late third instar larva and early pupal stages and, as for the other photoreceptors, the subcellular localization was mainly cytoplasmic and apical (Fig. 3K). Moreover, the enhancer trap line cdi^{BA01}, which has previously been used to describe the *cdi* expression pattern in CNS midline cells of *Drosophila* embryos (Matthews and Crews, 1999), showed expression in all ommatidial cells of the early pupal eye (Fig. 3L,M).

cdi is required for F-actin organization and apical-basal polarity of the nascent ommatidia

To understand the suppressive effect of *cdi* on sev^{S11}, we examined the effects of *cdi* overexpression on actin polymerization. We tested whether the *UAS-cdi* construct was able to inhibit actin depolymerization, a function that has already been described for the mammalian gene TESK1 (Toshima et al., 2001a). To this aim, we stained actin filaments with rhodamine-labeled phalloidin, which specifically binds to F-actin at the junction between subunits. We analyzed overexpression of *cdi* in clones generated with the flip-out technique (Ito et al., 1997) and found ectopic accumulation of F-actin in the cortex of cells overexpressing *cdi* both anterior and posterior to the morphogenetic furrow (Fig. 4A-C). Posterior to the morphogenetic furrow, where the ommatidial clusters are being assembled, F-actin is enriched at the apical tips of presumptive R cells in ommatidial preclusters of wild-type eyes (Pickup et al., 2002), possibly to concentrate signaling components that promote photoreceptor determination and spatial organization (Banerjee et al., 1987; Tomlinson et al., 1987; Van Vactor et al., 1991). In *cdi*-overexpressing cells, ectopic F-actin accumulation was extensive to all cells and even more pronounced at the apical region of the interacting precursors of the photoreceptor cells (Fig. 4D-F).

The apical constrictions of the developing ommatidial clusters are also enriched with junctional complexes, such as adherens junctions (Wolf and Ready, 1993). In *cdi* overexpressing cells, we did not find significant alterations of the concentration of both DE-cadherin and β-catenin, but these junctional proteins were found mislocalized and displaced towards a more basal position. Indeed, the apical areas where F-actin accumulates in the rhabdomere region were extended basally in *cdi*-overexpressing cells concomitantly with β-catenin domain displacement (Fig. 4F-G). In sections along the

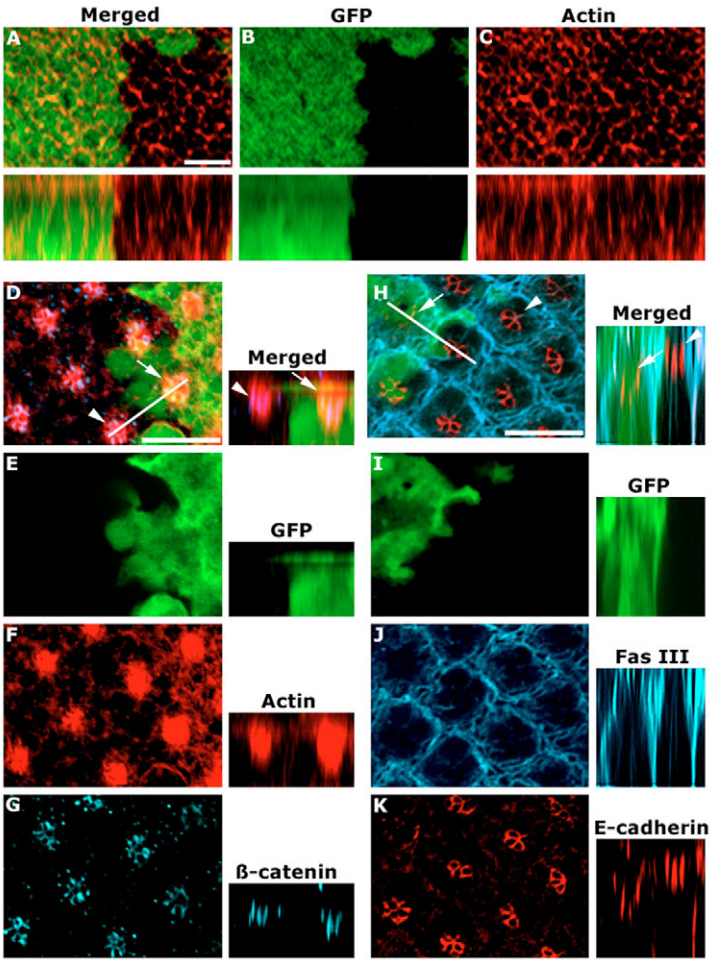

Fig. 4. Overexpression of *cdi* in eye discs. Clones of cells overexpressing *cdi* are labeled with GFP (green). (A-C) Clone anterior to the morphogenetic furrow where cells overexpressing *cdi* concentrate more F-actin (red) in the cell cortex. Upper panels show a cross-section, lower panels a transverse section. (D-G) Detail of a confocal cross-section at the apical region of developing ommatidia posterior to the morphogenetic furrow stained with phalloidin (red) and anti-β-catenin (blue). Note the F-actin accumulation in the *cdi*-overexpressing cells (F). Arrows point to a *cdi*-overexpressing ommatidial cluster and arrowhead to a wild-type cluster. Localization of β-catenin in *cdi*-overexpressing cells is displaced basally (G). Left panels: cross-sections. Right panels: transverse section through a mutant ommatidial cluster adjacent to a wild-type cluster. (H-K) Apical cross-section through ommatidial clusters stained with Fasciclin III (blue) and DE-cadherin (red). Note that the DE-cadherin of the closely apposed photoreceptor membranes in wild-type cells (arrowhead) is absent in the *cdi*-overexpressing ommatidial cluster (arrow). However, in a transverse section containing a cdi-overexpression cluster (arrow) next to a wild-type cluster (arrowhead), DE-cadherin is found more basally and in an abnormal arrangement (right panels). Fasciclin III, used to mark the cell contour, denotes that the *cdi*-overexpressing cluster is not shrunk or smaller. Diagonal lines in D and H indicate the region represented in the transverse sections. Bars, 10 μm.

apical-basal axis (transverse sections), confocal planes of mutant and wild-type ommatidial clusters showed an enlargement of the F-actin-enriched domain of the cluster and the β-catenin zone was displaced to a more basal position. The DE-cadherin in ectopically expressing *cdi* cells was located more basal in comparison to adjacent wild-type cells (Fig. 4H-K).

To further explore the role of *cdi* during eye development, we studied the loss-of-function phenotypes of *cdi* using the cdi^{R47} allele (Fig. 1E), which was generated after excision of a P-element insertion (Matthews and Crews, 1999; Raymond et al., 2004). We have molecularly characterized this allele and found that it lacks 2.077 bp uncovering the *mRpL55* gene and the first exon of *cdi*. Homozygous cdi^{R47} mutant embryos are lethal at the first larval instar. RT-PCR on these larvae showed that *cdi* and *mRpL55* transcripts were absent, whereas the mRNA of the nearby gene *ATP-syn-d* was present (data not shown). We also found that clones of cdi^{R47} cells removed the Cdi protein (Fig. 5A-C).

To avoid side-effects of *mRpL55*, we studied the phenotypes of *cdi* mutant discs with the cdi^{R47} mutation in a *GMR-Gal4 UAS-mRpL55* background to complement the loss of *mRpL55*. We first analyzed mutant clones in the eye imaginal disc and observed that F-actin distribution was irregular, granulated and disorganized (Fig. 5D-F). These effects were less evident in ommatidia that were composed of mutant and wild-type cells, especially when there was a nearby wild-type sector, which suggests a non-autonomous rescue of the overall organization. Conversely, ommatidia located in large mutant areas showed a strong perturbation of the actin network, either when the ommatidia were entirely mutant or when mosaic with few wild-type cells (Fig. 5D-F). To test whether the actin disorganization correlated with an alteration of the apical-basal polarity of the epithelium, we analyzed the localization of markers of the adherens junctions. We found that β-catenin and DE-cadherin in *cdi* mutant cells were displaced to a more basal position (Fig. 5G-J). These results show that the overall regular apical-basal organization of the photoreceptor cells is disrupted in mutant clones. To control whether these phenotypes are due to *cdi* loss-of-function, we generated clones of cdi^{r47} in a background overexpressing both *UAS-mRpL55* and *UAS-cdi* transgenes under *a GMR-Gal4* driver and found normal distribution of F-actin and apical localization of adherens junctions proteins (Fig. 5K-O).

Since we were unable to find cdi^{R47} mutant clones in adult eyes, we used Flp/FRT-driven mitotic recombination in a *Minute* background to give a proliferative advantage to the mutant cells (Morata and Ripoll, 1975). Even under these conditions, most of the adult eyes did not contain clones, and when they did, the clones were extremely reduced in size. Surviving mutant ommatidia had fewer and smaller photoreceptors than wild-type (Fig. 5P,Q). It could be that the

lethality of *cdi*^{R47} was due to the loss-of-function of *mRpL55* rather than of *cdi*, as it has been shown that *mRpL55* is required for cell viability in early embryos and pupal stages, and for cell cycle progression (Tselykh et al., 2005; Dimova et al., 2003). However, it has been described that mitotic clones of mutant *mRpL55* in the eye disc grow similarly to the corresponding wild-type twin clones, although mutant clones in the adult eye are absent (Tselykh et al., 2005). Thus the effects on viability in the adult eye could also be due to the lack of *mRpL55* during pupal stages, whereas it is likely that *cdi* is required for viability already at the larval stages. Indeed, clones of *cdi*^{R47} in a *UAS-mRpL55* background resulted in autonomous cell death, as assayed with cleaved caspase-3 antibody (Fig. 5R-T). Together these findings suggest that loss-of-function of *cdi* results in actin depolymerization and alteration of the epithelial condition, as inferred from adherens junctions markers, and that *cdi* mutant cells are eliminated from the epithelium through cell death.

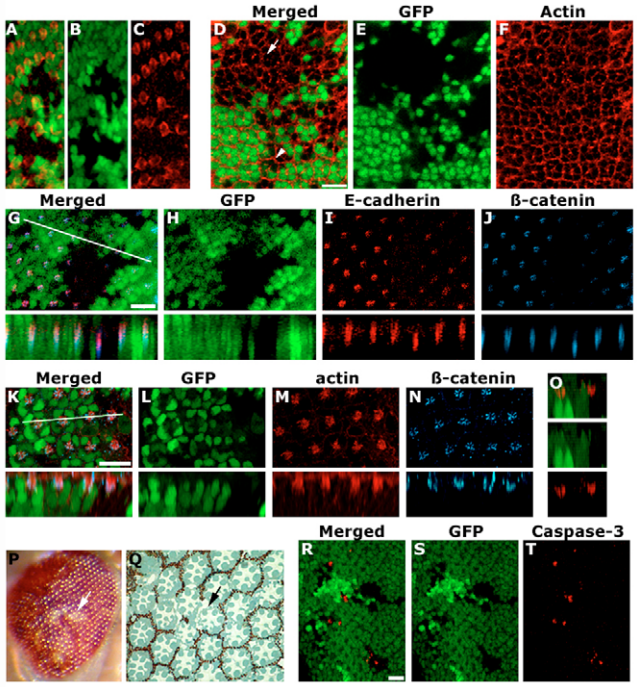

Fig. 5. Loss of *cdi* function in the developing eye. (A-C) Clones of *cdi*^{R47} (lack of GFP in A and B) show a lack of Cdi expression as assayed by anti-Cdi (red in A and C). The confocal image was taken at the level of inner photoreceptors of a late third instar larva where a transient accumulation of Cdi is found. (D-F) Mitotic clones of homozygous *cdi*^{R47} cells (lack of GFP). All these clones were supplied with *UAS-mRpL55* under *GMR-Gal4* driver. Actin organization is severely altered in mutant ommatidia (arrow). Clones containing both wild-type and mutant cells appear normal (arrowhead). (G-J) Clone of *cdi* mutant cells (lack of GFP) counterstained with anti-β-catenin (blue) and anti DE-cadherin (red). A single confocal cross-section (upper panels) taken at the level of the adherens junctions of the wild-type cells. Note that in this level of the mutant sector, both proteins are absent. Transverse section (lower panels) where β-catenin and DE-cadherin are aberrantly positioned. (K-N) Clones of *cdi*^{R47} cells (lack of GFP) complemented with the double transgene *UAS-mRpL55* and *UAS-cdi* under the *GMR-Gal4* driver and stained for phalloidin (red), and β-catenin (blue). (O) Transverse section of another clone (lack of GFP) as in K stained with DE-cadherin (red). Top, merged; middle, GFP; bottom, DE-cadherin. (P) Eye of a fly showing *cdi*^{R47} mutant clones (white sectors, arrow) in *Minute*$^{+}$ background. (Q) Semi-thin section of a mosaic eye, showing a clone of *cdi*^{R47} mutant ommatidia (absence of inter-ommatidial pigmentation; arrow points to mutant cells). (R-T) Clones of *cdi*^{R47} supplied with *UAS-mRpL55* and stained with anti-caspase-3. Thin lines represent the plane of transverse sectioning. Bars, 10 μm.

Actin turnover and signaling in ommatidial clusters

As mentioned above, *cdi* and LIMK phosphorylate ADF/cofilin to inactivate it and inhibit actin depolymerization. Conversely, ADF/cofilin is activated by dephosphorylation, which depends on the activity of a family of cofilin phosphatases such as *slingshot* (*ssh*). The loss-of-function of *ssh* causes F-actin accumulation (Niwa et al., 2002). If the gain-of-function of *cdi* is responsible for the perturbation of the signal transduction required for R7 specification, it should

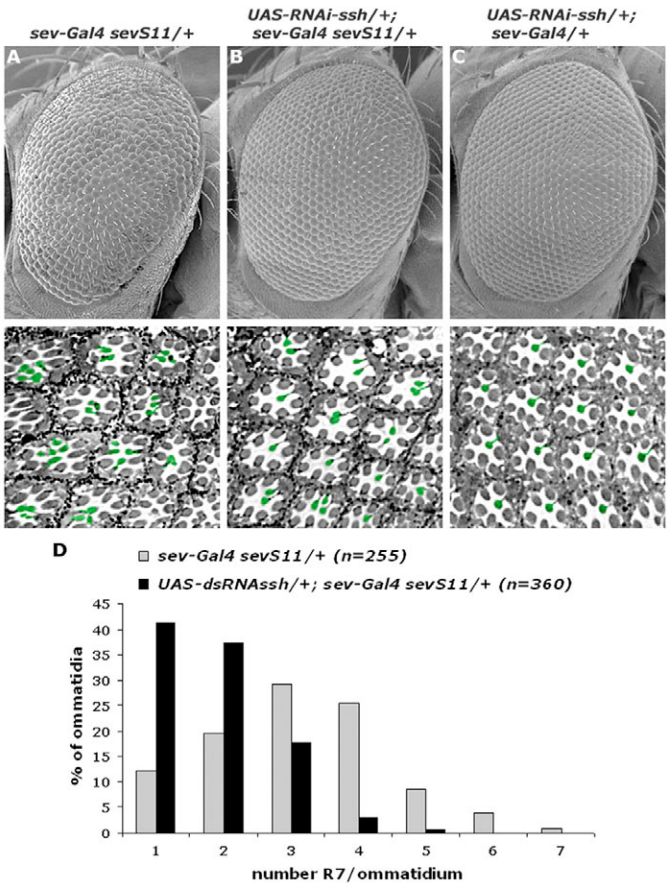

Fig. 6. *ssh* suppression of the activated Sev pathway. (A) Rough eye phenotype due to the *sev*^{S11} construct (*sev-Gal4 sev*^{S11}/+). (B) Suppression of the *sev*^{S11} rough eye phenotype when *UAS-RNAi-ssh* is activated (*UAS-RNAi-ssh/+; sev-Gal4 sev*^{S11}/+). (C) The activation of the transgene (*UAS-RNAi-ssh/+; sevGal4*) does not alter eye morphology. Upper panels: SEM images. Lower panels: tangential semi-thin sections with R7 photoreceptors colored green. (D) The histogram shows distribution profiles of the number of R7 photoreceptors per ommatidium for each genotype represented. The statistical analysis reveals significant differences between the genotypes (P<0.001).

be possible to mimic the suppression of R7 by inhibiting *ssh* function.

Actin turnover mediated by *ssh* seems to be essential for ommatidial assembly and *ssh*-null mosaic clones in the developing ommatidia of the third instar eye disc show apical accumulation of F-actin (Rogers et al., 2005). We tested whether the loss-of-function of *ssh* behaves similar to the gain-of-function of *cdi* in a background of activated Sev signaling. We generated flies containing the activated sev^{S11} construct and a *UAS* double-strand *RNAi-ssh* driven by *sev-Gal4*. In contrast to the use of loss-of-function mutants (Rogers et al., 2005), the activation of inducible RNAi did not alter eye morphology on its own (Fig. 6C), possibly due to a partial interference of *ssh* mRNA. In the sev^{S11} genetic background, the *sev-Gal4*-driven expression of *UAS-RNAi-ssh* resulted in suppression of the rough eye phenotype and a reduction of the number of extra R7 per ommatidium with an average of 1.8 R7 cells per omatidium in contrast to 3.1 in controls (*sev-Gal4* sev^{S11}), recapitulating the effects observed with overexpression of *cdi* (Fig. 6A,B). Similarly, the ADF/cofilin tsr^{2}/tsr^{ntf} hypomorphic heteroallelic combination also suppressed the sev^{S11} rough eye phonotype albeit weakly (2.7 R7 per ommatidium of tsr^{2}/tsr^{ntf}; sev^{S11}eyes; results not shown).

It has been shown that *ssh* co-localizes with the Sev RTK at the apical tips of the *sevenless* equivalence group, and that the distribution of Ssh is controlled by Sev. Interestingly, *ssh* null clones result in some, though slight, effects on the position of Sev in the equivalence group (Rogers et al., 2005). This opens the possibility that the localization of Sev could be fine-tuned by the Ssh and Cdi balance that drives actin organization, and that a shifting of the localization of the receptor could affect the transduction of the signal. The receptor Sev is also tightly localized at the apical tips of the *sevenless* equivalence group (Tomlinson et al., 1987), similarly to Boss in the tips of the R8 cells (Reinke and Zipursky, 1988). We explored whether alterations of *cdi* expression resulted in mislocalization of Sev RTK. To this aim, we generated gain- and loss-of-function clones of *cdi* and analyzed the distribution of Sev RTK protein along the apical-basal axis of the developing ommatidia. Clones ectopically expressing *cdi* showed an aberrant distribution of Sev, rather than fully apical (Fig. 7A-D). The loss of *cdi* function resulted in more severe defects, such as isolated particle distribution rather than concentrated at the apical tip (Fig. 7E-G) or low Sev RTK concentration, possibly due to cells entering apoptosis (Fig. 5R-T).

Discussion

We have identified *center divider* (*cdi*) in a misexpression screen for genes suppressing the rough eye phenotype induced by the gain-of-function of Sev RTK. The use of a *UAS-cdi* transgene confirmed the involvement of *cdi* in the sev^{S11} suppression. Moreover, the suppression of the Sev pathway by *cdi* observed when Boss ligand is overexpressed provides further evidence that *cdi* plays a role in modulating this pathway. *cdi/TESK1* kinases are required for the phosphorylation dependent inhibition of ADF/cofilin, and therefore inhibiting actin filament depolymerization (Toshima et al., 2001a). The results presented here illustrate that alterations of *cdi* expression result in a perturbation of the cortical F-actin network and the adherens junction complex, as DE-cadherin and β-catenin and ultimately the Sev RTK are mislocalized. Both adherens junction proteins are displaced when *cdi* is overexpressed but also when *cdi* is downregulated. This suggests that for the correct positioning of the apical adherens junctions in developing eye cells a balance between actin polymerization and depolymerization is required and that *cdi* is a key player in the regulation of that balance. We have also shown that the loss-of-function of *ssh*, which is the phosphatase responsible for the activation of ADF/cofilin, is suppressing the sev^{S11} phenotype.

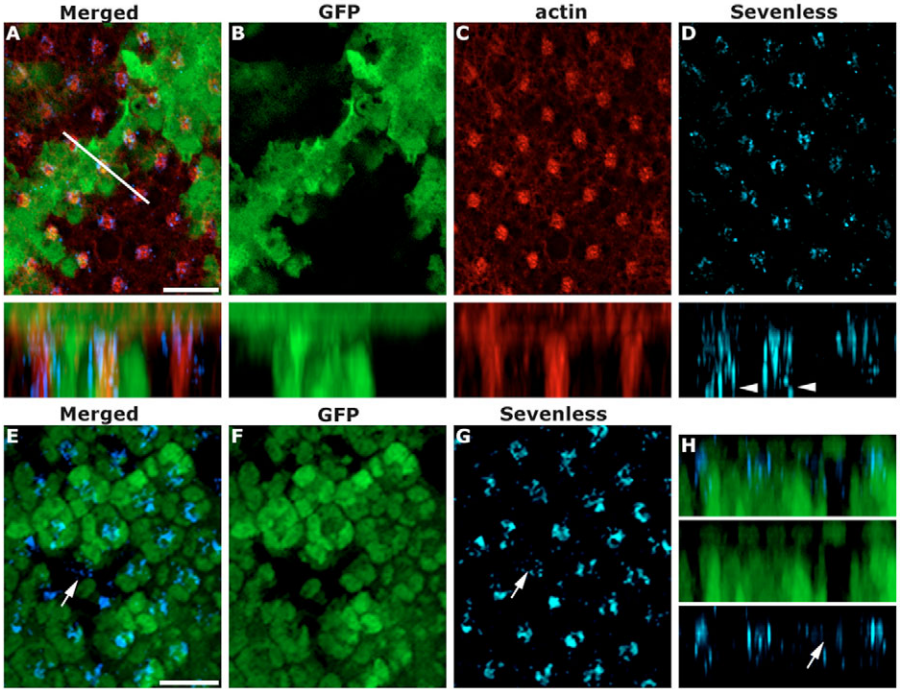

Fig. 7. Sev RTK localization in *cdi* gain- and loss-of-function clones. (A-D) Upper panels show a cross-section confocal image of *cdi* gain-of-function clones labeled with GFP (green) and F-actin (red). Lower panels show a transverse section of the same preparation taken through the region indicated with the white line in A. Sev RTK protein (blue) localization is extended to a more basal position in the mutant ommatidia (arrowheads). (E-G) Loss-of-function clone marked by the absence of GFP. Note that in some mutant ommatidia (arrow) Sev RTK (blue) staining is lower than in the wild-type. (H) Transverse sections of a loss-of-function clone where the Sev RTK staining (blue) of the apical membrane (arrow) is reduced. Bars, 10 μm.

cdi has been identified in several genetic screens to search for genes involved in neural development and signaling. *cdi* has also been found in an enhancer trap screen undertaken to identify genes involved in the embryonic central nervous system owing to its expression in all CNS midline primordial cells of the young embryo (Matthews and Crews, 1999; Kearney et al., 2004). Also an EP misexpression screen for genes that perturb axon guidance and synaptogenesis has revealed *cdi* as a candidate (Kraut et al., 2001). A screen for modifiers of activated RacGAP(84C) or its GTPase-activating protein (GAP) domain identified *cdi* as an effector of Rac1 (Raymond et al., 2004). The ectopic expression of *cdi* also suppresses the rough eye phenotype caused by the loss of rhabdomeres, abnormal photoreceptor cells and polarity defects, induced by a dominant negative form of the small GTPase Rac1, RacN17 (Raymond et al., 2004). Moreover, the mammalian homolog TESK1 has been shown to be activated upon matrix adhesion and is regulated by binding of 14-3-3 protein and sprouty4 (Toshima et al., 2001b; Tsumura et al., 2005). TESK1 has been isolated in a two-hybrid screen as a partner of sprouty 4, and the TESK1-sprouty4 interaction has been confirmed by co-immunoprecipitation (Leeksma et al., 2002). In *Drosophila sprouty* acts as a negative regulator of the Ras/MAPK signaling pathway (Casci et al., 1999; Reich et al., 1999; Kramer et al., 1999), and it is thought that its mammalian homolog will act similarly (Leeksma et al., 2002). This raises the possibility that *cdi/TESK1* could act as a crosstalk between Ras/MAPK and small GTPase signaling cascades.

The overall organization of the epithelium in the developing eye undergoes cellular rearrangements from late third instar to pupal stages (Cagan and Ready, 1989). This includes cell shape changes that transform the single layered epithelium into the functional assembly of all cells in the adult ommatidia. These rearrangements are tightly associated with an axial actin cytoskeleton in the rhabdomeral microvilli, which extends into the cytoplasm of the photoreceptor cells (Arikawa et al., 1990; Drenckhahn and Dermietzel, 1988). Depletion of F-actin in *hindsight* mutant eyes is associated with abnormal photoreceptor morphology and apical-basal polarity (Pickup et al., 2002). Furthermore, cells mutant for *twinstar*, which encodes the fly homolog of ADF/cofilin, produce planar cell polarity defects in the developing eye (Blair et al., 2006). The link between morphogenesis and cytoskeleton that establishes the regular ommatidial architecture has been thoroughly studied for elements of the adherens junctions. An example is *canoe*, a PDZ-domain protein homologous to the mammalian AF-6/afadin that binds to actin filaments (Yamamoto et al., 1997; Mandai et al., 1997) and is associated with the cytoplasmic side of the adherens junctions (Matsuo et al., 1999). Canoe protein is involved in the fine-tuning of Ras1 activity by direct binding to the N-terminus of Ras1 (Matsuo et al., 1997). Adherens junctions are necessary for ommatidial architecture as overexpression of the *canoe* transgene driven by the *sevenless* enhancer causes split or missing photoreceptors (Matsuo et al., 1999), and both loss-of-function and ectopic expression can induce aberrant ommatidial orientation (Gaengel and Mlodzik, 2003). Also βH-spectrin, which tightly co-localizes with DE-cadherin, is essential for the production of R7 (Thomas et al., 1998).

The suppression of the ligand-independent activation of the Sev pathway by *cdi* shown here suggests that cytoarchitecture rearrangements due to ectopic *cdi* impede the straight intracellular transduction of the signal. The localization of the receptor, or of a downstream transduction protein such as Son of Sevenless (Sos) or Ras, is essential for the reliability of the pathway (reviewed in Ebisuya et al., 2005). Because no obvious suppression of the activated Ras or Raf constructs by *cdi* overexpression was observed (data not shown), we propose that the cytoskeletal organization targets either the anchoring of the receptor or of a protein interacting with the receptor. Recent findings show that glutamate receptors, in the fly neuromuscular junction, are anchored to the actin cytoskeleton by the Coracle protein, as disruption of actin or Coracle results in depletion of A-type receptors (Chen et al., 2005a). Also the multidomain scaffold protein Paxillin facilitates the formation of the Raf-MEK-ERK complex at the focal adhesions, where actin filament ends are anchored, as described for hepatocyte growth factor (HGF)-stimulated epithelial cells (Ishibe et al., 2003). In *Drosophila*, the *paxillin* overexpression phenotype is rescued by ectopic *cdi* and *cdi* has been identified as a target of *paxillin*-mediated Rho GTPase regulation (Chen et al., 2005b). Because Cdi-mediated actin arrangements affect Sev RTK localization and function, we propose that the reliability of the Sev RTK signaling pathway is dependent on cytoskeleton and adherens junctions, illustrating how the truthful integration of cell structure, adhesion and signaling is necessary for normal development.

In wild-type discs, F-actin is enriched at the apical tips of presumptive R cells. This apical F-actin forms part of a tightly localized signaling complex enriched for receptor and ligand molecules, such as Sev RTK (Banerjee et al., 1987; Tomlinson et al., 1987) and Boss (Van Vactor et al., 1991), as well as other interacting molecules such as Delta-Notch (Fehon et al., 1991; Kooh et al., 1993). Interestingly, the ligand-independent activation of Sev RTK sev^{S11} in the subpopulation of ommatidial cells also shows localization of the activated tyrosine kinase domain in the apical region of the cells, similarly to wild-type Sev (Basler et al., 1991). The perturbation of cellular architecture in the apical region of the mutant photoreceptor precursors would have serious consequences on the correct positioning of cells in the epithelium, on the apposition of interacting membranes and on the proper subcellular localization of pathway components, resulting in a disruption of cell fate. In this context, appropriate balance of actin organization by Ssh (Rogers et al., 2005) and Cdi through their regulation of ADF/cofilin will be crucial for Sev localization and transduction. This is strengthened by the observation that the loss of the fly ADF/cofilin *twinstar* reduces, although weakly, the number of R7s in the sev^{S11} eyes. Thus, overexpression of Cdi, by either EP elements or UAS transgenes, results in a mislocalization of Sev, which affects the transduction of the signal. Therefore, we conclude that fine-tuning of the actin turnover is fundamental to execute the program that drives R7 identity.

Materials and Methods

Fly stocks

The activated Sev RTK construct *yw;* sev^{S11} (Basler et al., 1991) and recombinant flies *sev-Gal4* sev^{S11}*/TM3* were used for the screening and genetic interactions. The EP lines *EP(33-077)*, *EP(34-165)* and *EP(44-004)* were identified among 5000 insertions of a double-headed EP element (Fig. 1C; H.S., D. Nellen, K. Basler and E.H., unpublished). Plasmid rescue revealed that they are inserted 1800 bp, 2045 bp and 2963 bp, respectively, upstream of the predicted ATG of *mRpL55* (GadFly

database). The UAS sites at the 5′ end of the EPs were excised by *Cre-loxP*-mediated recombination to yield single-headed EP elements capable of driving *cdi* and *mRpL55*. The following transgenes and mutations were used for interaction studies and expression pattern: *UAS-boss* (a gift of H. Kramer, UT Southwestern Medical Center, Dallas, TX), *sev-Gal4* (Rintelen et al., 2003); heat shock-Gal4 (*hs-Gal4)*, *en-Gal4* (from K. Basler, University of Zürich, Zürich, Switzerland), *GMR-Gal4* (Hay et al., 1994), *UAS-ssh-dsRNA* (Niwa et al., 2002), tsr^{2} and tsr^{ntf}*/TSTL* (Chen et al., 2001), *yw hs-Flp 1.22; P[Act5C<FRTy+FRT>Gal4]* (Ito et al., 1997), enhancer trap cdi^{BA01} for *cdi* expression pattern and cdi^{R47} for loss-of-function studies (Matthews and Crews, 1999). Fly cultures and crosses were grown on standard fly medium at 25°C, except for the genetic interaction between *twinstar* (*tsr)* and sev^{S11} that was carried out at 18°C.

Clonal analysis

cdi loss-of-function clones were generated using the FLP/FRT system (Xu and Rubin, 1993). Flies *yw hs-Flp; FRT82 Ubi-GFP/TM6B* were crossed to *yw; FRT82B* cdi^{R47}*/TM6B* and clones in the eye discs of the progeny were induced by 20 minutes heat shock at 37°C at 50±4hours after egg laying (AEL). *UAS-mRpL55*^{T14} was used to complement the loss of *mRpL55* of the cdi^{R47} mutation using *GMR-Gal4*. To obtain *Minute*$^{+}$ clones (Morata and Ripoll, 1975) in the adult eye the marker stock used was *yw hsFlp; FRT82B M(3)* w^{+}*/TM6By*$^{+}$ and crossed with the *FRT82B* cdi^{R47}*/TM6B* flies. The heat shock was carried out for 30 minutes at 37°C (80±5 hours AEL). Control tissue in the adult eye contained pigment granules due to the presence of a functional w^{+} transgene.

For ectopic expression, clones were generated by means of the 'FLP-out' technique using the line *yw hs-Flp 1.22; P[Act5C<FRTy+FRT>Gal4]* P[*UAS-GFP]/CyO* crossed to *UAS-cdi* flies. Larvae were heat-shocked at 37°C for 10 minutes at 50±4 hours AEL.

Molecular characterization of the cdi^{R47} allele

To generate a sequencing template we used a pair of primers (forward: 5′-gtcgcgctcataaattcttctac-3′ and reverse: 5′-gcctctgcaaccaacacttaca-3′) flanking the genetically mapped deletion breakpoints (Matthews and Crews, 1999). We sequenced it using the same primers in order to molecularly define the breakpoints of this 2.077 bp deletion that uncovers the first exon of *cdi* and the *mRpL55* gene.

Semi-quantitative RT-PCR

Total RNA from control *EP/hs-Gal4* 98±5h AEL larvae (without heat shock), RNA from the experimental *EP/hs-Gal4* 98±5h AEL larvae (heat shock for 1 hour at 37°C at 96±5 h), and RNA from wild-type and cdi^{R47} first instar larvae were extracted using Trizol Reagent (Gibco-BRL). cDNA was synthesized with the MMLV-Reverse Transcriptase (Invitrogen) from 1 μg of RNA in order to amplify by PCR, with specific primers, the following transcripts: *cdi* (5′-acgacgcgggcatctttcacagg-3′ and 5′-gacttgctccggccgacgactc-3′); *mRpL55* (5′-caggctgcatcgctcggttta-3′ and 5′-cgggcctccaatctcgctctg-3′); *rp49* as a control (5′-agtatctgtgcccaacatcg-3′ and 5′-ttccaccaggttacaagaac-3′); *ATPsyn-d* (5′-cggcgccttcaagaccaagtcg-3′ and 5′-tttgggtaatttacttcaacgcg-3′).

Plasmid construction and transgenic flies generation

The 4.7 kb *cdi* cDNA with the entire open reading frame was obtained from an adult cDNA library in lambdaZap (a gift from S. Ekengren, Stockholm University, Stockholm, Sweden) and sequenced on both strands. The *cdi* cDNA was cloned with *Not*I and *Xho*I restriction enzymes into the pUAST vector (Brand and Perrimon, 1993).

The *UAS-mRpL55* transgene was generated by inserting the full-length *mRpL55* cDNA sequence from a cDNA clone (RH10246; Berkeley *Drosophila* Genome Project) into the pUAST vector. Germ line transformations were carried out using w^{1118} as the host strain.

Scanning electron microscopy and histology

Flies were dehydrated in 25, 50, 75, 95 and 100% ethanol for 24 hours each to prepare samples for scanning electron microscopy (SEM). To get rid of accumulated debris in the eyes, the flies were sonicated for 30 seconds in an ultrasound bath followed by a final change of 100% ethanol. Flies were critical-point dried and coated with gold to be examined in a Leica 360 scanning microscope.

Adult eyes were fixed and embedded in Spurr's medium as previously described (Basler and Hafen, 1988). Semi-thin sections were obtained and stained with methylene blue for analysis under a Leica DMLB microscope. For each genotypic combination, ommatidia from 3 to 5 different eyes were counted. A Chi-square test on contingency tables was performed. This allowed us to see significant differences in number of R7 per ommatidium comparing control versus experimental flies.

Antibodies and immunohistochemistry

Antibody staining on imaginal discs was carried out using a standard protocol. Primary antibodies used in this study were: rabbit anti-Cdi (1:1000, kindly provided by C. Samakovlis, Wenner-Gren Institute, Stockholm, Sweden), rabbit anti β-galactosidase (1:1000, Cappel), mouse anti-Boss (1:2000, gift from L. Zipursky, University of California, Los Angeles, CA), mouse anti-Prospero (1:4, Developmental Studies Hybridoma Bank, DSHB), rat anti-DE-cadherin (1:50, DSHB), mouse anti-armadillo (anti-β-catenin) (1:50, DSHB), rabbit anti-cleaved caspase-3 (1:100, Cell Signaling Technologies), mouse anti-Sev (1:5000 a gift of M. Simon, Stanford University, Stanford, CA) and mouse anti-FasciclinIII (1:1000, a gift of D. Brower, University of Arizona, Tucson, AZ). Secondary antibodies were obtained from Jackson Immuno Research and include: donkey anti-rat-Rhodamine Red (1:200), goat anti-mouse-FITC (1:200), goat anti-mouse-Cy5 (1:200) and donkey anti-rabbit-Rhodamine Red (1:200). To stain the actin cytoskeleton, Rhodamine-coupled phalloidin (Molecular Probes) was used at 1:40 dilution for 30 minutes after disc fixation. Nuclei were stained with Sytox-green (1:5000, Molecular Probes).

Imaging

Double and triple fluorochrome-labeled samples were analyzed and captured using Leica TCS and Olympus confocal microscopes. Images were processed using the ImageJ (NIH). Stacks of confocal images were re-sliced to produce digital transverse (XZ) sections. Final artwork was processed by Adobe Photoshop 7.0 software.

We thank D. Nellen and K. Basler for their help and discussions. To M. Simon for providing the anti-Sev. We thank C. Samakovlis, P. Wuestemann and A. Boehne for their help. We are grateful to H. Kramer, T. Uemura, S. Crews, J. F. De Celis, F. Laski, J. Settleman and Bloomington Stock Center for fly stocks. Special thanks to M. Morey for critically reading the manuscript. We also acknowledge Developmental Studies Hybridoma Bank for antibodies requested. M.S. is the recipient of a fellowship from Universitat de Barcelona. This work was supported by the Ministerio de Ciencia y Tecnologia and Ministerio de Educación y Ciencia (Spain) (grant BMC2003-05018 and BFU2004-04732) and an EMBO short term fellowship to F.S.

References

Arikawa, K., Hicks, J. L. and Williams, D. S. (1990). Identification of actin filaments in the rhabdomeral microvilli of Drosophila photoreceptors. *J. Cell. Biol* **110**, 1993-1998.

Banerjee, U., Renfranz, P. J., Hinton, D. R., Rabin, B. A. and Benzer, S. (1987). The sevenless+ protein is expressed apically in cell membranes of developing Drosophila retina; it is not restricted to cell R7. *Cell* **51**, 151-158.

Basler, K. and Hafen, E. (1988). Control of photoreceptor cell fate by the sevenless protein requires a functional tyrosine kinase domain. *Cell* **54**, 299-311.

Basler, K., Christen, B. and Hafen, E. (1991). Ligand-independent activation of the sevenless receptor tyrosine kinase changes the fate of cells in the developing Drosophila eye. *Cell* **64**, 1069-1081.

Blair, A., Tomlinson, A., Pham, H., Gunsalus, K. C., Goldberg, M. L. and Laski, F. A. (2006). Twinstar, the Drosophila homolog of cofilin/ADF, is required for planar cell polarity patterning. *Development* **133**, 1789-1797.

Brand, A. H. and Perrimon, N. (1993). Targeted gene expression as a means of altering cell fates and generating dominant phenotypes. *Development* **118**, 401-415.

Cagan, R. L. and Ready, D. F. (1989). The emergence of order in the Drosophila pupal retina. *Dev. Biol.* **136**, 346-362.

Casci, T., Vinos, J. and Freeman, M. (1999). Sprouty, an intracellular inhibitor of Ras signaling. *Cell* **96**, 655-665.

Chen, J., Godt, D., Gunsalus, K., Kiss, I., Goldberg, M. and Laski, F. A. (2001). Cofilin/ADF is required for cell motility during Drosophila ovary development and oogenesis. *Nat. Cell. Biol.* **3**, 204-209.

Chen, K., Merino, C., Sigrist, S. J. and Featherstone, D. E. (2005a). The 4.1 protein coracle mediates subunit-selective anchoring of Drosophila glutamate receptors to the postsynaptic actin cytoskeleton. *J. Neurosci.* **25**, 6667-6675.

Chen, G. C., Turano, B., Ruest, P. J., Hagel, M., Settleman, J. and Thomas, S. M. (2005b). Regulation of Rho and Rac signaling to the actin cytoskeleton by paxillin during Drosophila development. *Mol. Cell. Biol.* **25**, 979-987.

DesMarais, V., Ghosh, M., Eddy, R. and Condeelis, J. (2005). Cofilin takes the lead. *J. Cell. Sci.* **118**, 19-26.

Dimova, D. K., Stevaux, O., Frolov, M. V. and Dyson, N. J. (2003). Cell cycle-dependent and cell cycle-independent control of transcription by the Drosophila E2F/RB pathway. *Genes. Dev.* **17**, 2308-2320.

Drenckhahn, D. and Dermietzel, R. (1988). Organization of the actin filament cytoskeleton in the intestinal brush border: a quantitative and qualitative immunoelectron microscope study. *J. Cell. Biol.* **107**, 1037-1048.

Ebisuya, M., Kondoh, K. and Nishida, E. (2005). The duration, magnitude and compartmentalization of ERK MAP kinase activity: mechanisms for providing signaling specificity. *J. Cell. Sci.* **118**, 2997-3002.

Fehon, R. G., Johansen, K., Rebay, I. and Artavanis-Tsakonas, S. (1991). Complex cellular and subcellular regulation of notch expression during embryonic and imaginal development of Drosophila: implications for notch function. *J. Cell. Biol.* **113**, 657-669.

Freeman, M. (1996). Reiterative use of the EGF receptor triggers differentiation of all cell types in the Drosophila eye. *Cell* **87**, 651-660.

Gaengel, K. and Mlodzik, M. (2003). Egfr signaling regulates ommatidial rotation and cell motility in the Drosophila eye via MAPK/Pnt signaling and the Ras effector Canoe/AF6. *Development* **130**, 5413-5423.

Ghosh, M., Song, X., Mouneimne, G., Sidani, M., Lawrence, D. S. and Condeelis, J. S. (2004). Cofilin promotes actin polymerization and defines the direction of cell motility. *Science* **304**, 743-746.

Gohla, A., Birkenfeld, J. and Bokoch, G. M. (2005). Chronophin, a novel HAD-type serine protein phosphatase, regulates cofilin-dependent actin dynamics. *Nat. Cell. Biol.* **7**, 21-29.

Hafen, E., Basler, K., Edstroem, J. E. and Rubin, G. M. (1987). Sevenless, a cell-specific homeotic gene of Drosophila, encodes a putative transmembrane receptor with a tyrosine kinase domain. *Science* **236**, 55-63.

Hart, A. C., Kramer, H., Van Vactor, D. L., Jr, Paidhungat, M. and Zipursky, S. L. (1990). Induction of cell fate in the Drosophila retina: the bride of sevenless protein is predicted to contain a large extracellular domain and seven transmembrane segments. *Genes. Dev.* **4**, 1835-1847.

Hay, B. A., Wolff, T. and Rubin, G. M. (1994). Expression of baculovirus P35 prevents cell death in Drosophila. *Development* **120**, 2121-2129.

Ishibe, S., Joly, D., Zhu, X. and Cantley, L. G. (2003). Phosphorylation-dependent paxillin-ERK association mediates hepatocyte growth factor-stimulated epithelial morphogenesis. *Mol. Cell* **12**, 1275-1285.

Ito, K., Sass, H., Urban, J., Hofbauer, A. and Schneuwly, S. (1997). GAL4-responsive UAS-tau as a tool for studying the anatomy and development of the Drosophila central nervous system. *Cell. Tissue. Res* **290**, 1-10.

Izaddoost, S., Nam, S. C., Bhat, M. A., Bellen, H. J. and Choi, K. W. (2002). Drosophila Crumbs is a positional cue in photoreceptor adherens junctions and rhabdomeres. *Nature* **416**, 178-183.

Kearney, J. B., Wheeler, S. R., Estes, P., Parente, B. and Crews, S. T. (2004). Gene expression profiling of the developing Drosophila CNS midline cells. *Dev. Biol.* **275**, 473-492.

Kooh, P. J., Fehon, R. G. and Muskavitch, M. A. (1993). Implications of dynamic patterns of Delta and Notch expression for cellular interactions during Drosophila development. *Development* **117**, 493-507.

Kramer, S., Okabe, M., Hacohen, N., Krasnow, M. A. and Hiromi, Y. (1999). Sprouty: a common antagonist of FGF and EGF signaling pathways in Drosophila. *Development* **126**, 2515-2525.

Kraut, R., Menon, K. and Zinn, K. (2001). A gain-of-function screen for genes controlling motor axon guidance and synaptogenesis in Drosophila. *Curr. Biol.* **11**, 417-430.

Leeksma, O. C., Van Achterberg, T. A., Tsumura, Y., Toshima, J., Eldering, E., Kroes, W. G., Mellink, C., Spaargaren, M., Mizuno, K., Pannekoek, H. et al. (2002). Human sprouty 4, a new ras antagonist on 5q31, interacts with the dual specificity kinase TESK1. *Eur. J. Biochem.* **269**, 2546-2556.

Mandai, K., Nakanishi, H., Satoh, A., Obaishi, H., Wada, M., Nishioka, H., Itoh, M., Mizoguchi, A., Aoki, T., Fujimoto, T. et al. (1997). Afadin: A novel actin filament-binding protein with one PDZ domain localized at cadherin-based cell-to-cell adherens junction. *J. Cell. Biol.* **139**, 517-528.

Matsuo, T., Takahashi, K., Kondo, S., Kaibuchi, K. and Yamamoto, D. (1997). Regulation of cone cell formation by Canoe and Ras in the developing Drosophila eye. *Development* **124**, 2671-2680.

Matsuo, T., Takahashi, K., Suzuki, E. and Yamamoto, D. (1999). The Canoe protein is necessary in adherens junctions for development of ommatidial architecture in the Drosophila compound eye. *Cell. Tissue. Res.* **298**, 397-404.

Matthews, B. B. and Crews, S. T. (1999). Drosophila center divider gene is expressed in CNS midline cells and encodes a developmentally regulated protein kinase orthologous to human TESK1. *DNA Cell. Biol.* **18**, 435-448.

Morata, G. and Ripoll, P. (1975). Minutes: mutants of drosophila autonomously affecting cell division rate. *Dev. Biol.* **42**, 211-221.

Muralidhar, M. G., Callahan, C. A. and Thomas, J. B. (1993). Single-minded regulation of genes in the embryonic midline of the Drosophila central nervous system. *Mech. Dev.* **41**, 129-138.

Niwa, R., Nagata-Ohashi, K., Takeichi, M., Mizuno, K. and Uemura, T. (2002). Control of actin reorganization by Slingshot, a family of phosphatases that dephosphorylate ADF/cofilin. *Cell* **108**, 233-246.

Pellikka, M., Tanentzapf, G., Pinto, M., Smith, C., McGlade, C. J., Ready, D. F. and Tepass, U. (2002). Crumbs, the Drosophila homologue of human CRB1/RP12, is essential for photoreceptor morphogenesis. *Nature* **416**, 143-149.

Pickup, A. T., Lamka, M. L., Sun, Q., Yip, M. L. and Lipshitz, H. D. (2002). Control of photoreceptor cell morphology, planar polarity and epithelial integrity during Drosophila eye development. *Development* **129**, 2247-2258.

Raymond, K., Bergeret, E., Avet-Rochex, A., Griffin-Shea, R. and Fauvarque, M. O. (2004). A screen for modifiers of RacGAP(84C) gain-of-function in the Drosophila eye revealed the LIM kinase Cdi/TESK1 as a downstream effector of Rac1 during spermatogenesis. *J. Cell. Sci.* **117**, 2777-2789.

Ready, D. F., Hanson, T. E. and Benzer, S. (1976). Development of the Drosophila retina, a neurocrystalline lattice. *Dev. Biol* **53**, 217-240.

Reich, A., Sapir, A. and Shilo, B. (1999). Sprouty is a general inhibitor of receptor tyrosine kinase signaling. *Development* **126**, 4139-4147.

Reinke, R. and Zipursky, S. L. (1988). Cell-cell interaction in the Drosophila retina: the bride of sevenless gene is required in photoreceptor cell R8 for R7 cell development. *Cell* **55**, 321-330.

Rintelen, F., Hafen, E. and Nairz, K. (2003). The Drosophila dual-specificity ERK phosphatase DMKP3 cooperates with the ERK tyrosine phosphatase PTP-ER. *Development* **130**, 3479-3490.

Rogers, E. M., Hsiung, F., Rodrigues, A. B. and Moses, K. (2005). Slingshot cofilin phosphatase localization is regulated by Receptor Tyrosine Kinases and regulates cytoskeletal structure in the developing Drosophila eye. *Mech. Dev.* **122**, 1194-1205.

Tepass, U., Tanentzapf, G., Ward, R. and Fehon, R. (2001). Epithelial cell polarity and cell junctions in Drosophila. *Annu. Rev. Genet.* **35**, 747-784.

Thomas, G. H., Zarnescu, D. C., Juedes, A. E., Bales, M. A., Londergan, A., Korte, C. C. and Kiehart, D. P. (1998). Drosophila betaHeavy-spectrin is essential for development and contributes to specific cell fates in the eye. *Development* **125**, 2125-2134.

Tomlinson, A. and Ready, D. F. (1986). Sevenless a cell-specific homeotic mutation of the Drosophila eye. *Science.* **231**, 400-402.

Tomlinson, A. and Ready, D. F. (1987). Neuronal differentiation in the Drosophila ommatidium. *Dev. Biol.* **120**, 366-376.

Tomlinson, A., Bowtell, D. D., Hafen, E. and Rubin, G. M. (1987). Localization of the sevenless protein, a putative receptor for positional information, in the eye imaginal disc of Drosophila. *Cell* **51**, 143-150.

Toshima, J., Ohashi, K., Okano, I., Nunoue, K., Kishioka, M., Kuma, K., Miyata, T., Hirai, M., Baba, T. and Mizuno, K. (1995). Identification and characterization of a novel protein kinase, TESK1, specifically expressed in testicular germ cells. *J. Biol. Chem.* **270**, 31331-31337.

Toshima, J., Toshima, J. Y., Amano, T., Yang, N., Narumiya, S. and Mizuno, K. (2001a). Cofilin phosphorylation by protein kinase testicular protein kinase 1 and its role in integrin-mediated actin reorganization and focal adhesion formation. *Mol. Biol. Cell* **12**, 1131-1145.

Toshima, J. Y., Toshima, J., Watanabe, T. and Mizuno, K. (2001b). Binding of 14-3-3beta regulates the kinase activity and subcellular localization of testicular protein kinase 1. *J. Biol. Chem.* **276**, 43471-43481.

Tselykh, T. V., Roos, C. and Heino, T. I. (2005). The mitochondrial ribosome-specific MrpL55 protein is essential in Drosophila and dynamically required during development. *Exp. Cell. Res.* **307**, 354-366.

Tsumura, Y., Toshima, J., Leeksma, O. C., Ohashi, K. and Mizuno, K. (2005). Sprouty-4 negatively regulates cell spreading by inhibiting the kinase activity of testicular protein kinase. *Biochem. J.* **387**, 627-637.

Van Vactor, D. L., Jr, Cagan, R. L., Kramer, H. and Zipursky, S. L. (1991). Induction in the developing compound eye of Drosophila: multiple mechanisms restrict R7 induction to a single retinal precursor cell. *Cell* **67**, 1145-1155.

Wolff, T. and Ready, D. F. (1991). The beginning of pattern formation in the Drosophila compound eye: the morphogenetic furrow and the second mitotic wave. *Development* **113**, 841-850.

Wolff, T. and Ready, D. F. (1993). Pattern formation in the Drosophila retina. In *The Development of Drosophila melanogaster* (ed. M. Bate and A. Martinez Arias), pp. 1277-1325. Cold Spring Harbor Laboratory Press.

Woods, D. F., Wu, J. W. and Bryant, P. J. (1997). Localization of proteins to the apico-lateral junctions of Drosophila epithelia. *Dev. Genet.* **20**, 111-118.

Xu, T. and Rubin, G. M. (1993). Analysis of genetic mosaics in developing and adult Drosophila tissues. *Development* **117**, 1223-1237.

Yamamoto, T., Harada, N., Kano, K., Taya, S., Canaani, E., Matsuura, Y., Mizoguchi, A., Ide, C. and Kaibuchi, K. (1997). The Ras target AF-6 interacts with ZO-1 and serves as a peripheral component of tight junctions in epithelial cells. *J. Cell. Biol.* **139**, 785-795.